

# Low-Leakage $\text{In}_{0.53}\text{Ga}_{0.47}\text{As}$ p-i-n Photodetector Fabricated on GaAs Substrate with Linearly Graded Metamorphic $\text{In}_x\text{Ga}_{1-x}\text{P}$ Buffer

Chi-Kuan Lin, Hao-Chung Kuo, Yu-Sheng Liao, and Gong-Ru Lin\*

Department of Photonics & Institute of Electro-Optical Engineering  
National Chiao Tung University  
No. 1001, Ta Hsueh Rd., Hsinchu, Taiwan 30050, R. O. C.

## ABSTRACT

A novel top-illuminated metamorphic  $\text{In}_{0.53}\text{Ga}_{0.47}\text{As}$  p-i-n photodiodes (MM-PINPD) grown on GaAs substrate by using a linearly graded  $\text{In}_x\text{Ga}_{1-x}\text{P}$  ( $x$  graded from 0.51 to 1) buffer layer is reported. The dark current, optical responsivities, noise equivalent power (NEP), and operational bandwidth of the MM-PINPD with aperture diameter of 60  $\mu\text{m}$  are 13 pA, 0.77/0.59 (1310/1550 nm) A/W,  $6.9 \times 10^{-11}$  W/Hz<sup>1/2</sup>, and 7.5 GHz, respectively. The performances of the MM-PINPD on GaAs are demonstrated to be better than those of a similar device made on InGaAs/InP substrate.

**Keywords:** Metamorphic, InGaAs, heterostructure, p-i-n photodiode, GaAs.

## 1. INTRODUCTION

Long-wavelength photodiodes with  $\text{In}_{0.53}\text{Ga}_{0.47}\text{As}$  absorption layer for fiber-optic communication networks have been fabricated on the lattice-matched InP substrate over several decades the years. However, InP suffers from several drawbacks including higher fragility, less mature processing technologies, and smaller available wafer sizes comparing to GaAs. Recently, the metamorphic epitaxy has emerged to enable the growth of  $\text{In}_{0.53}\text{Ga}_{0.47}\text{As}$ -based optoelectronic devices such as photodiodes and high electron mobility transistors on GaAs substrates. Compositionally graded metamorphic buffer layers are extensively utilized to accommodate large lattice mismatch between a semiconductor substrate and epitaxial layers, which overcomes the limitation of band-gap engineering imposed by the substrate lattice parameters. Threading dislocations and defects are mainly confined within the metamorphic buffer without propagating vertically into the device layer. Technically, the metamorphic epitaxy facilitates some advantages from greater strength, no need of InP substrate, ready availability of large diameter substrates, easier material handling, and the compatibility with existing manufacturing infrastructure. These lead to a cost effective solution without sacrificing device performance. Previously, some researchers have devoted the metamorphic-epitaxial growth by introducing various materials to grow the buffer layer on GaAs substrate, which has been successfully applied to the fabrication of metamorphic p-i-n photodetector (MM-PINPD).<sup>1-3</sup> Jang et al. demonstrated an MM-PINPD with a linearly graded InAlGaAs buffer layer and  $\text{p}^+\text{-InGaAs/InGaAs/n}^+\text{-InAlAs}$  p-i-n structure<sup>1</sup>, in which the  $\text{In}_{1-x-y}\text{Ga}_x\text{Al}_y\text{As}$  layer serves as a lattice-constant transformer between the GaAs substrate and the  $\text{In}_{0.53}\text{Ga}_{0.47}\text{As}$  layers. By using such a metamorphic buffer, an InGaAs PINPD with a very low dark current density of  $3.4 \times 10^{-4}$  A/cm<sup>2</sup> at bias of 5 V and an optical responsivity of 0.55 A/W at 1.55  $\mu\text{m}$  was reported. Up to now, versatile aluminum-contained material systems have been proposed for the growth of graded buffer layers on GaAs substrate, however, the aluminum containing layers in the optoelectronic devices are known to exhibit problems such as deep traps and rapid oxidation. Recently, few studies were carried out to replace Al-contained materials by using InGaP as the buffer layer<sup>2</sup> with its lattice constant gradually varying from that of GaP to that of InP. The use of InGaP graded layer thus benefits from the possibility of growing InP-based heterostructures on GaAs, GaP and Si substrate. Moreover, the transition between the graded buffer ( $\text{In}_x\text{Ga}_{1-x}\text{P}$ ,  $0 < x < 1$ ) and the InP layer can be very smooth since there is no compositional control problem in the InGaP/InP system. This is unlike the case of AlInAs or InGaAs buffer layers, where the switching of As to P at the interface usually generates a thin ternary or quaternary interfacial layer. Furthermore, since the bandgap of InGaP is larger than that of InP, a fully transparent buffer layer can be achieved, which is advantageous for long-wavelength optoelectronic devices. Nonetheless, few characteristics of InGaP/GaAs systems for optoelectronic applications were

\*grlin@faculty.nctu.edu.tw; phone: 886-3-5712121 ext.56376; fax: 886-3-5716631

reported the first metamorphic InGaP-buffer based heterojunction bipolar transistors (HBT).<sup>3</sup> In this paper, we report the fabrication of top-illuminated metamorphic p-i-n photodiodes (MM-PINPD) grown on GaAs substrates using linearly graded In<sub>x</sub>Ga<sub>1-x</sub>P buffer layer. The demonstrated technique is particularly suitable for high mass-production of such devices on GaAs substrates. Dark currents, responsivities, and operational bandwidths of the MM-PINPD with an aperture diameter of 60 μm are reported.

## 2. FABRICATION AND EXPERIMENT SETUP

The MM-PIN heterostructure was grown on a 3-in (100)-oriented n-type GaAs substrate using gas source molecular beam epitaxy, as shown in Fig. 1. A buffer layer consisting of 1.5 μm-thick undoped In<sub>x</sub>Ga<sub>1-x</sub>P (x linearly gradually changed from 0.51 to 1) was grown at 500°C. Afterwards, the PINPD with structure of n<sup>+</sup>-InP (1 μm)/undoped InP (0.5 μm)/undoped In<sub>0.53</sub>Ga<sub>0.47</sub>As (2.5 μm)/undoped InP (1 μm) were grown upon the MM layer at 600°C. A p-type InP ohmic contact layer was formed using standard Zn diffusion into up-doped InP window layer, and a 0.8-μm-thick Ti-Au metal was evaporated on the pad with diameter of >80 μm. A Si<sub>3</sub>N<sub>4</sub> dielectric layer was deposited on the active region (with diameter of 60 μm) of the MM-PINPD device surface for passivation and antireflection. The active area of the MM-PINPD was laterally isolated from the rest of the wafer by a reactive-ion-etched trench, and was vertically isolated by a high bandgap cladding layer.

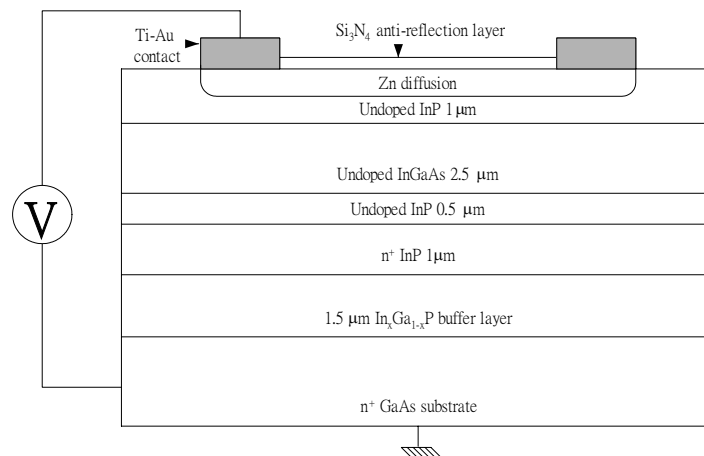


Fig. 1: The layer structure of an MM-PINPD on GaAs.

The MM-PINPD chip was mounted on a SMA connector with its n-type GaAs substrate connecting to the pin of SMA. A metal probe was employed to negatively bias the p-type contact on MM-PINPD. The capacitance of the MM-PINPD with SMA mount was measured by a capacitance-voltage meter (Hewlett Packard, 4280A). The current-voltage response was measured using a programmable electrometer (Keithley, model 6517) with resolution as low as 100 fA. The power-dependent photocurrent and wavelength-dependent optical responsivity ranged from 1310-nm to 1550-nm were determined using tunable lasers (Hewlett Packard, 8168F) and distributed feedback laser diodes (DFBLDs) in connection with an attenuator (JDS-FITEL, HA9). For high-speed performance, the DFBLDs were gain-switched to generate a pulse-train with full width at half maximum (FWHM) of 42 ps at repeating rate of 1GHz. The temporal response of the MM-PINPD was monitored on a digital sampling oscilloscope (DSO, Hewlett Packard, 86100A+86109B). The setup illustration and picture are shown below (see Figs. 2 and 3).

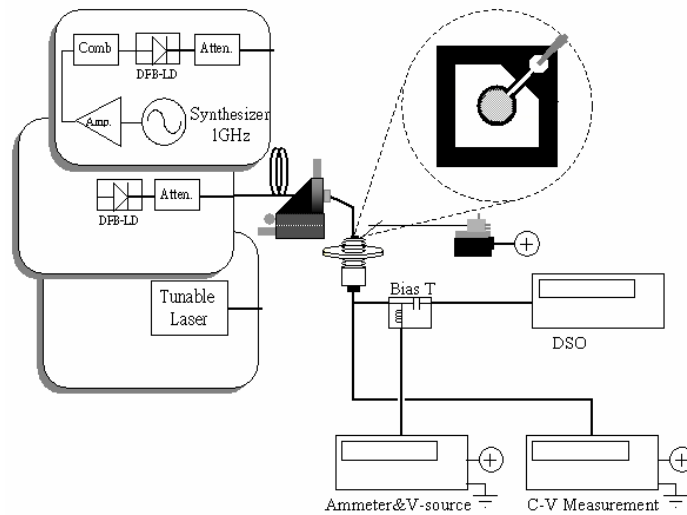


Fig. 2: The light-emitted and electrical measurement diagram of measured setup.

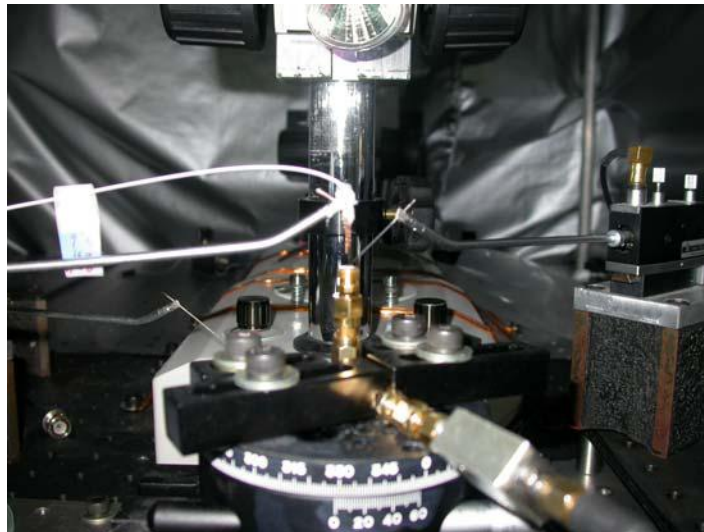


Fig. 3: The lightwave probe based testing bench.

### 3. RESULTS AND DISCUSSION

The surface morphology of the epilayers was *in-situ* controlled by monitoring the reflection high energy electron diffraction (RHEED) pattern. The composition, structural quality and degree of strain relaxation were subsequently evaluated by high-resolution x-ray diffraction (HRXRD) and the cross-section TEM image. In Fig. 4, the cross-section view of the metamorphic buffer layer micrograph taken by transmission electron microscope (TEM) shows a dense dislocation network that is necessarily formed during the grading to expand the lattice constant.



Fig. 4: Cross-sectional TEM photograph of a linearly-graded  $\text{In}_x\text{Ga}_{1-x}\text{P}$  metamorphic buffer layer.

In general, a thick InGaP buffer layer can generate a high density of defects that results in high dark currents because of the unfiltered lattice-mismatch strain and the difference in its thermal expansion coefficients to the GaAs substrate. Therefore, the magnitude of dark currents could reflect the quality of InGaP metamorphic layer. The density of dislocations predominantly contained in the metamorphic buffer layer of  $1 \times 10^6 \text{ cm}^{-2}$  was estimated from the plane-view photography of TEM. The device layers upon the metamorphic buffer are nearly dislocation-free (with density of  $1 \times 10^6 \text{ cm}^{-2}$ ). The current-voltage (I-V) response of the negatively biased MM-PINPD with 60- $\mu\text{m}$  diameter is plotted in Fig. 5. Even with the metamorphic layer, an extremely low dark current of 13 pA is obtained at bias voltage of -5 V, which is comparable to that of a similar PINPD made on InP substrate. The corresponding leakage current density of  $3.6 \times 10^{-7} \text{ A/cm}^2$  is almost three orders of magnitude smaller than that with a  $\text{p}^+\text{-InGaAs/InGaAs/n}^+\text{-InAlAs}$  p-i-n structure made on an InAlGaAs buffered GaAs substrate.<sup>1</sup> Such a low dark current reveals the better lattice-matching property between the InGaP buffer and the GaAs substrate as compared to the InAlGaAs system.

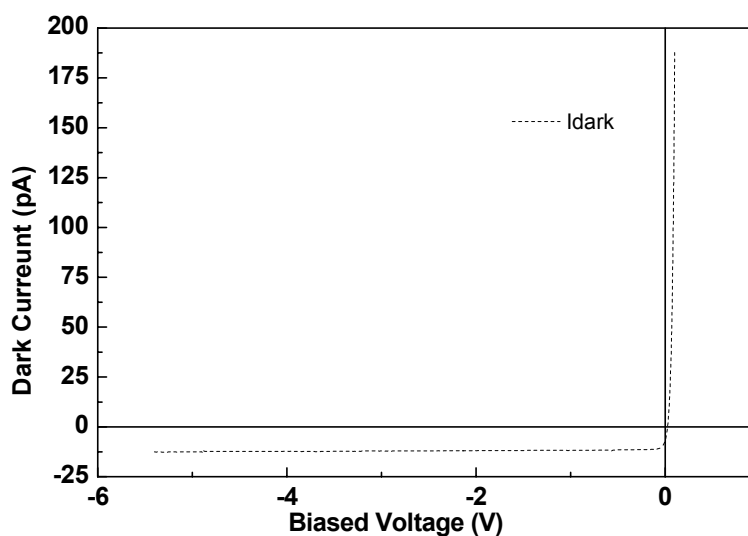


Fig. 5: Dark current versus biased voltage from -5 V to 0.1 V for MM-PINPD. The leakage current is 13 pA at -5V.

The power- and bias-dependent photocurrent of MM-PINPD illuminated at 1550-nm wavelength is shown plotted in the Fig. 6. At a reverse bias of 5 V, The photocurrents measured at illuminating power of 0 dBm is 595  $\mu$ A, corresponding to an optical responsivity of 0.6 A/W. The photocurrent of MM-PINPD decreases from 0.6 mA to 0.6 nA as the illuminating power attenuates from 0 dBm to -60 dBm, while a linear relationship between the illuminating power and corresponding photocurrent is found, as shown in Fig. 7.

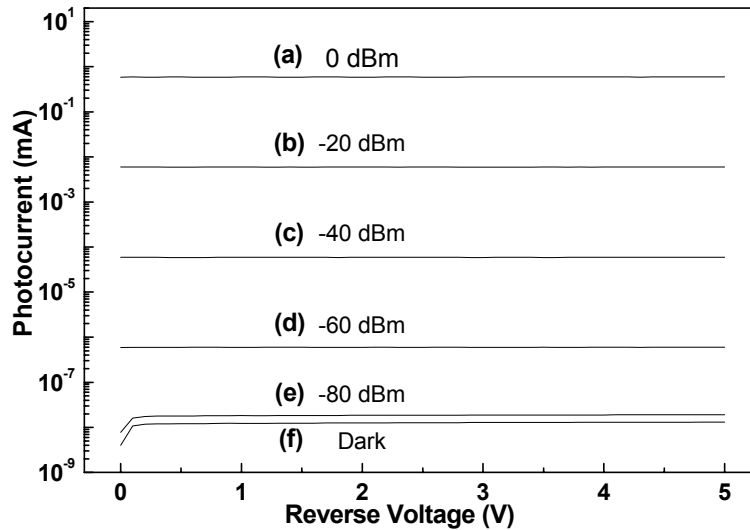


Fig. 6: The photocurrent variations of the MM-PINPD under 1550-nm CW light injection from 0 dBm to -80 dBm with 20 dBm increment.

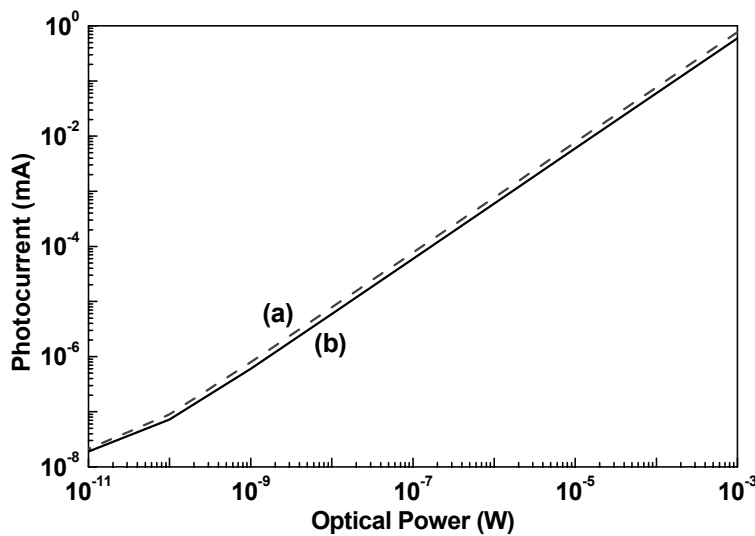


Fig. 7: The photocurrent variations of the MM-PINPD versus different optical injection power at (a) 1310-nm wavelength and; (b) 1550-nm wavelength.

The transferred function of the MM-PINPD is extremely linear, which is even detectable at illuminating power of below 100 pW due to its extremely low dark current. Moreover, the photocurrents and optical responsivities at 1310 nm and 1550 nm were also compared in Fig. 8.

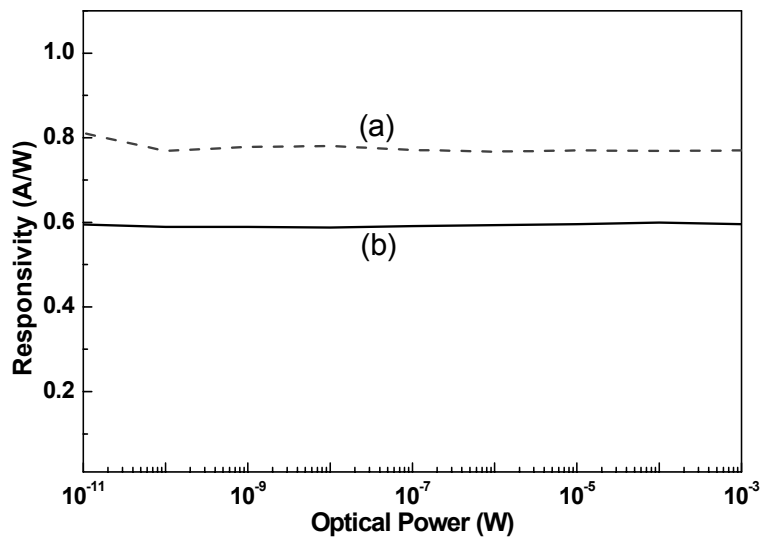


Fig. 8: The optical responsivities of the MM-PINPD as a function of optical injection power at (a) 1310-nm wavelength; (b) 1550-nm wavelength.

The optical responsivity  $R$  of the MM-PINPD is calculated using  $R = (I_{ph} - I_d)/P_{laser}$ , where  $I_{ph}$  and  $I_d$  denote the photocurrent and dark current of the MM-PINPD, and  $P_{laser}$  is the laser power at the illuminating end. Under an illuminating power of 0 dBm, the optical responsivities at 1310 nm and 1550 nm are 0.77 and 0.59 (A/W), respectively. The optical responsivities are also higher than those of a similar double-heterojunction PINPD made on InAlGaAs buffered GaAs substrate<sup>1</sup>.

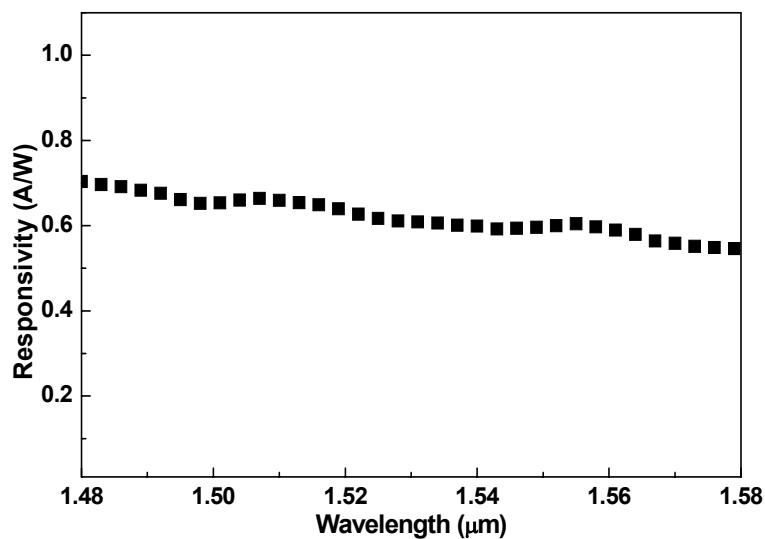


Fig. 9: The optical responsivity of the MM-PINPD as a function of wavelength.

Nonetheless, the data reported in Figs. 6 to 9 have not yet corrected for reflection losses at the air-substrate interface. The tuning of illuminating wavelength from 1480 nm to 1580 nm reveals a decreasing trend in responsivity (from 0.6 to 0.77 A/W), which is almost identical to the conventional  $In_{0.53}Ga_{0.47}As$  PINPD fabricated on InP substrate.

The capacitance (C) and the load resistance (r) of the MM-PINPD with SMA mount measured at bias of -5 V are 0.525 pF and 1 MΩ, which corresponds to a theoretically calculated 3 dB bandwidth of  $3 \times 10^5$  Hz. The shot and thermal noises of the MM-PINPD are calculated as  $1.1 \times 10^{-12}$  A and  $6.9 \times 10^{-11}$  A, respectively. The shot noise  $i_I$  is calculated by using  $i_I = (2eI_d B)^{0.5}$ , where e is the electron charge,  $I_d$  is the dark current, and B is the 3 dB operational bandwidth of  $B = 1/(2\pi rC)$  with r and C denoting the load resistance and capacitance of MM-PINPD, respectively. On the other hand, the thermal noise  $i_R$  is calculated by using  $i_R = (4kTB/r)^{0.5}$ , where k is the Boltzmann constant, T is the absolute temperature, B is the 3 dB operational bandwidth, and r is the load resistance. The noise equivalent power (NEP, defined as  $NEP = I_n/R$ , the ratio of detected noise current to the responsivity) of the MM-PINPD is thus dominated by the thermal noise. Consequently, the NEP at 1550 nm and 1310 nm are 117.4 pW/Hz<sup>1/2</sup> and 90 pW/Hz<sup>1/2</sup>, respectively. These correspond to the detectivity (defined as  $D = 1/NEP$ ) values at 1550 nm and 1310 nm of  $8.5 \times 10^9$  Hz<sup>1/2</sup>/W and  $1.1 \times 10^{10}$  Hz<sup>1/2</sup>/W, respectively. In comparison, these results are comparable or even better than those of a commercial PINPD (Edmund, InGaAs PINPD, model 155-753), as listed in Table I.

	diameter (μm)	R (A/W) (1.31/1.55 μm)	NEP (W/Hz <sup>1/2</sup> )	t <sub>r</sub> (ps) (max)	I <sub>d</sub> (pA)	C (pF)
Edmund InGaAs PD	70	0.9/0.95	$2.8 \times 10^{-14}$	200	30	0.75
MM-PINPD	60	0.77/0.59	$6.9 \times 10^{-11}$	52	13	0.53

Table I: The parametric comparison on the diameter, responsivity (R), NEP, rise time (t<sub>r</sub>), dark current (I<sub>d</sub>), and capacitance (C) between the MM-PINPD and the commercial product (Edmund's InGaAs PD)

By using a gain-switched DFBLD with of pulsewidth 42 ps and average power 0.1 mW at repeating rate of 1 GHz, the switching responses of the MM-PINPD corresponding to 1310-, and 1550-nm pulses, respectively, are also shown in the Fig. 10. There are multi-reflection signals observed as the gradually decaying side peaks in the temporal response, which is mainly attributed to the absence of the transimpedance amplifier (TIA) on SMA mount.

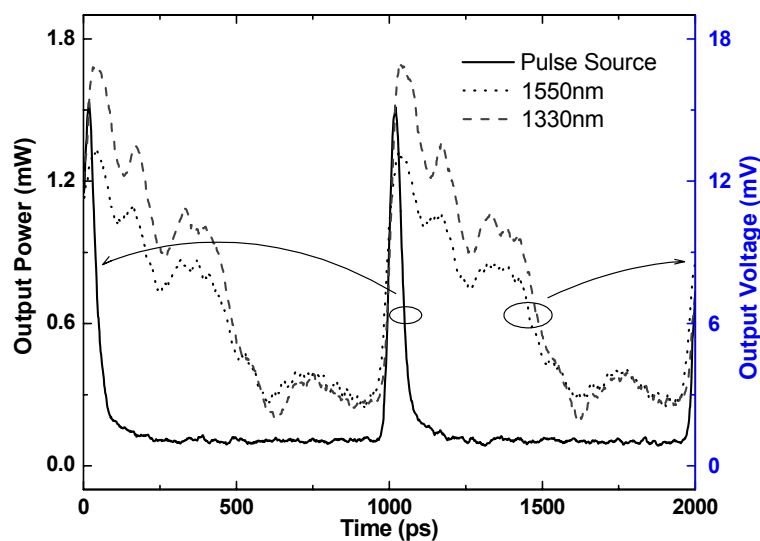


Fig. 10: The figure shows the temporal traces of the MM-PINPD at 1310 nm and 1550 nm under the illumination of a gain-switched DFBLD at repetition frequency of 1 GHz.

Nevertheless, it is notable that MM-PINPD has excellence performance on rise time. The rising time of the MM-PINPD illuminated at 1310 nm and 1550 nm are 35.56 ps and 51.85 ps, respectively. The switching time is less than 250 ps. A Fourier transform of the pulsed response depicts that the operational bandwidth of the MM-PINPD can be up to 7.5 GHz even without any impedance mating circuitry, as shown in Fig. 11. Temporal and eye diagram analyses of the received pseudo-random binary sequence data corroborates that the MM-PINPD is promising for receiving the SONET/SDH protocol at a bit rate up to 2.5 Gbit/s or higher.

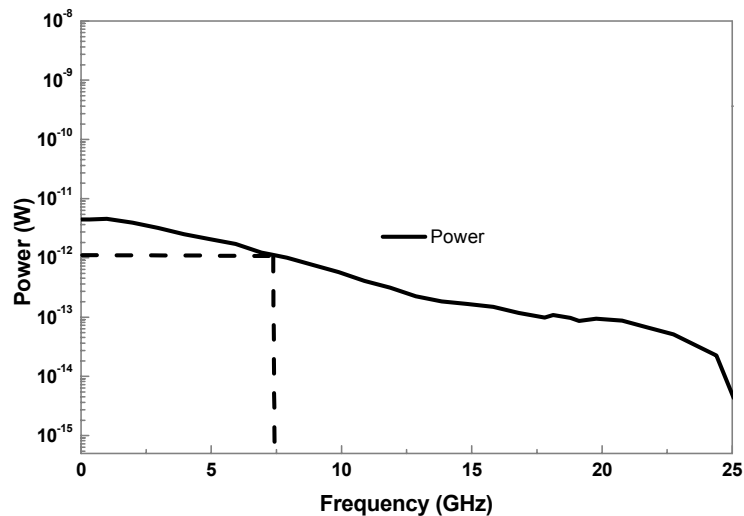


Fig. 11: The Fourier transformed frequency response of the pulsed response of the MM-PINPD at 1550 nm.

#### 4. CONCLUSION

Low-Leakage  $\text{In}_{0.53}\text{Ga}_{0.47}\text{As}$  p-i-n photodetector fabricated on GaAs substrate with linearly graded metamorphic  $\text{In}_x\text{Ga}_{1-x}\text{P}$  buffer layer have been demonstrated. The dc and radio frequency performance of the photodiodes are characterized. At bias of -5 V, the MM-PINPD exhibits a dark current of only 13 pA. The optical responsivities of 0.77 A/W and 0.59 A/W, and the NEP of  $90 \text{ pW/Hz}^{1/2}$  and  $117.4 \text{ pW/Hz}^{1/2}$ , respectively, are determined at 1310 nm and 1550 nm. All parameters are comparable to those of similar devices made on InP substrate or other InGaAs products epitaxial on an InGaAlAs buffered GaAs substrate. The operational bandwidth can be up to 7.5 GHz without reducing the diameter of aperture and conquering the reflected signal by impedance matching.

#### ACKNOWLEDGEMENT

This work was supported in part by National Science Council under grant NSC93-2215-E-009-007.

#### REFERENCES

1. J. H. Jang, and G. Cueva, D. C. Dumka, W. E. Hoke, P. J. Lemonias, and I. Adesida, "Long-Wavelength  $\text{In}_{0.53}\text{Ga}_{0.47}\text{As}$  Metamorphic p-i-n Photodiodes on GaAs Substrates," IEEE Photon. Technol. Lett., vol. 13, pp. 151-153, 2001.
2. T. P. Chin, H. Q. Hou, C. W. Tu, J. C. P. Chang and N. Otsuka, "InGaAs/InP and InAsP/InP quantum well structures on GaAs (100) with a linearly graded InGaP buffer layer grown by gas-source molecular beam epitaxy," Appl. Phys. Lett., vol. 64, pp. 2001-2003, 1994.
3. K. Yuan, K. Radhakrishnan, H. Q. Zheng, and G. I. Ng, "Metamorphic  $\text{In}_{0.52}\text{Al}_{0.48}\text{As}/\text{In}_{0.53}\text{Ga}_{0.47}\text{As}$  high electron mobility transistors on GaAs with  $\text{In}_x\text{Ga}_{1-x}\text{P}$  graded buffer," J. Vac. Sci. Technol. B, vol. 19, pp. 2119-2122, 2001.